Correlation of neural activity with behavioral kinematics reveals distinct sensory encoding and evidence accumulation processes during active tactile sensing

Ioannis Delis [a], Jacek P. Dmochowski [b], Paul Sajda [a,c,*], Qi Wang [a,*]

[a] Department of Biomedical Engineering, Columbia University, New York, NY, 10027, USA
[b] Department of Biomedical Engineering, City College of New York, New York, NY, 10031, USA
[c] Data Science Institute, Columbia University, New York, NY, 10027, USA

A B S T R A C T

Many real-world decisions rely on active sensing, a dynamic process for directing our sensors (e.g. eyes or fingers) across a stimulus to maximize information gain. Though ecologically pervasive, limited work has focused on identifying neural correlates of the active sensing process. In tactile perception, we often make decisions about an object/surface by actively exploring its shape/texture. Here we investigate the neural correlates of active tactile decision-making by simultaneously measuring electroencephalography (EEG) and finger kinematics while subjects interrogated a haptic surface to make perceptual judgments. Since sensorimotor behavior underlies decision formation in active sensing tasks, we hypothesized that the neural correlates of decision-related processes would be detectable by relating active sensing to neural activity. Novel brain-behavior correlation analysis revealed that three distinct EEG components, localizing to right-lateralized occipital cortex (LOC), middle frontal gyrus (MFG), and supplementary motor area (SMA), respectively, were coupled with active sensing as their activity significantly correlated with finger kinematics. To probe the functional role of these components, we fit their single-trial-couplings to decision-making performance using a hierarchical-drift-diffusion-model (HDDM), revealing that the LOC modulated the encoding of the tactile stimulus whereas the MFG predicted the rate of information integration towards a choice. Interestingly, the MFG disappeared from components uncovered from control subjects performing active sensing but not required to make perceptual decisions. By uncovering the neural correlates of distinct stimulus encoding and evidence accumulation processes, this study delineated, for the first time, the functional role of cortical areas in active tactile decision-making.

Introduction

Perceptual decisions rely on the integration of sensory evidence from the environment (Heekeren et al., 2004; Hanks and Summerfield, 2017). The quality of sensory evidence depends highly on our actions, as our movements affect how we sample, process and integrate information from the external world (Najemnik and Geisler, 2005; Renninger et al., 2007; Navalpakkam et al., 2010; Schroeder et al., 2010; Chukoskie et al., 2013; Toscani et al., 2013; Yang et al., 2016a; Tomassini et al., 2017; Tomassini and D'Ausilio, 2017). Hence, to optimize the speed and accuracy of our perceptual decisions we need to direct our actions so as to efficiently gather sensory information, a process called active sensing (Kleinfeld et al., 2006; Yang et al., 2016b). Importantly, the processing of sensory information acquired actively and its translation into perceptual

choices requires the interaction of multiple neural processes (and consequently multiple brain areas) over time (Philiastides and Sajda, 2006, 2007; Heekeren et al., 2008; Summerfield and de Lange, 2014; Rahnev et al., 2016). However, despite recent scientific interest in active sensing and decision-making, its neural underpinnings remain poorly understood.

Here we address this gap using a response-time active tactile decision-making task in which we simultaneously measured the electroencephalogram (EEG), active sensing behavior (movement kinematics) and task performance (accuracy and response time - RT) of subjects, the goal being to uncover the patterns of neural activity and sensorimotor behavior that drive active perceptual decisions.

To achieve this goal, we proceed in two steps. We first aim to characterize prominent components of active sensing brain entrainment. To
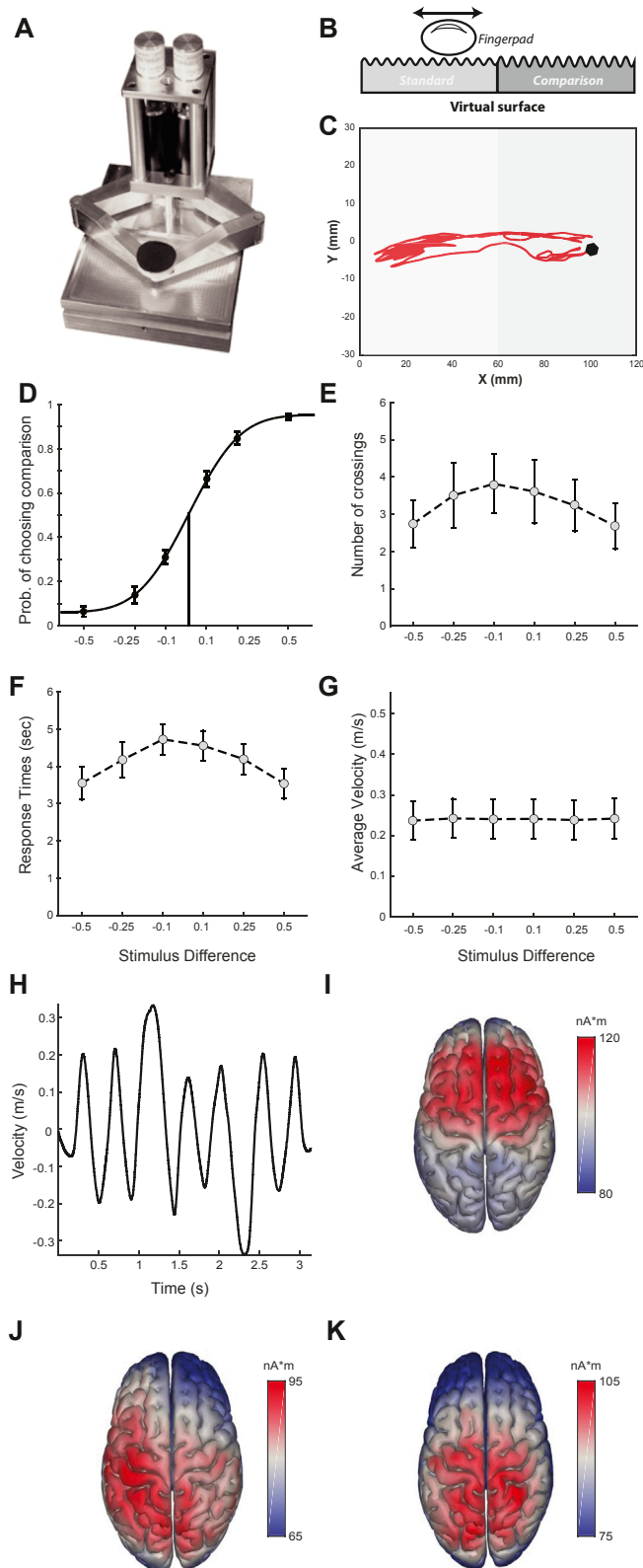
Fig. 1. Experimental design, behavioral results and principal components of EEG signals. A. The Pantograph is a haptic device used to render virtual surfaces that can be actively sensed. B. The stimulus. We programmed the Pantograph to generate a virtual grating texture. The workspace was split into two subspaces (left - L and right - R) that differed in the amplitude of the virtual surface that the subjects actively sensed. One of the two sides (randomly assigned) had the reference amplitude (equal to 1) and the other had the comparison amplitude that varied on each trial taking one of the values: 0.5, 0.75, 0.9, 1.1, 1.25, and 1.5. C. Index finger trajectory indicating the scanning pattern of the virtual texture in one trial. The two red dots indicate the starting point and endpoint. On this trial, the subject actively sensed the left subspace first, then moved to the right subspace and explored it before coming back to the left subspace again and reporting their choice. D. Psychometric curve indicating the percentage of non-reference choices for all stimulus differences. Dots indicate average proportion of choices across subjects and errorbars are standard error of the means (sem) across subjects. Data are fit using a cumulative Gaussian function. E. Response times for all stimulus differences shown as averages (sem) across subjects. F. Number of crossings (i.e. switchings between the two stimuli) for all stimulus differences shown as averages (sem) across subjects. G. Average finger velocities for all stimulus differences shown as averages (sem) across subjects. H. Velocity profile of the finger movement during the example trial. I-J-K. Brain sources of the first three principal components of the recorded EEG signals across subjects.

this end, we correlate the recorded EEG signals with the behavioral kinematics and extract components of neural activity coupled with components of sensorimotor behavior. Specifically, we hypothesize that changes in the speed with which subjects explore the tactile stimulus are indicative of the strategy they employ for acquiring and accumulating perceptual information and thus reflect active sensing behavior. Hence, we use the velocity profiles of the finger movements performed on each trial as correlates of the EEG recordings in order to uncover the neural underpinnings of active tactile sensing. The main advantage of this methodology is that it replaces unspecific measures of neural activations with measures that directly quantify the coupling between the components of continuous finger movement and brain activity, thereby tapping more directly into the neural correlates of tactile active exploration.

We further hypothesize that one's active sensing behavior, and the neural activity that underlies it, provides a view into the processes leading to decision formation. Thus, we ask if the perceptual, cognitive and motor processes involved in active tactile decision-making are modulated by the strength of the identified brain-behavior couplings. To dissect the constituent processes of decision-making during active sensing we employ a hierarchical drift diffusion model (HDDM) analysis. To assess if these processes bear any relation to the extracted brain-behavior correlated components, we integrate the HDDM with a regression analysis that uses the brain-behavior correlations as predictors for the HDDM parameters. The HDDM framework therefore provides a principled approach to investigate whether the neural representations of active tactile sensory processing drive decision formation and enables one to identify which of its integral processes may be predictive of behavior. Ultimately, we find that two distinct processes, namely tactile stimulus encoding and evidence accumulation, are driven by two distinct components of brain-behavior coupling.

Materials and methods

Active tactile texture discrimination task

Fifteen healthy right-handed subjects (6 female, aged 26 2 years) performed a two-alternative forced choice (2AFC) texture discrimination task during which they had to compare the amplitudes of two sinusoidal textures of the same frequency. All experimental procedures have been reviewed and approved by the Institutional Review Board (IRB) at Columbia University.

Subjects performed the task using a haptic device, called a Pantograph (Campion et al., 2005; Frissen et al., 2012), which can be

judiciously programmed to generate tactile sensations that resemble exploring real surfaces (see Fig. 1A). For this binary discrimination task, the workspace of the Pantograph (of dimensions 110 mm   60 mm) was split into two subspaces (left - L and right - R, 55 mm   60 mm each) and subjects experienced continuous sinusoidal forces of different amplitudes (but same wavelength of 10 mm) in the two subspaces (Fig. 1B). Subjects were asked to report as quickly and as accurately as possible which of the two subspaces had the higher texture amplitude. They placed their right index finger on the plate of the Pantograph, which was hidden behind a black curtain, and were allowed to move it freely in the Pantograph workspace to explore the textures of both subspaces before reporting their choice by pressing one of two buttons on a keyboard (left arrow for L, right arrow for R). During the experiment, the curtain blocked the subjects' view to their fingers, the subjects had no other visual input and were instructed to fixate on the keyboard they used to report their choices.

On each trial, subjects compared between the reference amplitude 1 (presented either on the left or right subspace) and one of six other amplitude levels (0.5, 0.75, 0.9, 1.1, 1.25, 1.5). Each subject performed 20 trials for each amplitude level, resulting in 20 trials x 6 amplitudes = 120 trials in total. The full experiment was split into 3 blocks of 40 trials. One subject showed poor behavioral performance (accuracy was not significantly different from chance level) and another subject's EEG recordings were significantly contaminated with eye movement artifacts, thus data from these two subjects were removed from any subsequent analyses. We report results from the remaining 13 subjects.

Control experiment

We recruited ten healthy right-handed subjects (4 females, aged 24   2 years) that were naïve to the experimental setup and the tactile discrimination experiment described above, and asked them to participate in a second experiment. The subjects were asked to actively explore the virtual surface generated by the Pantograph using their right index finger. During the experiment, the participants experienced the same tactile stimulation as for the tactile discrimination task, i.e. continuous sinusoidal forces of different amplitudes in the two subspaces, but, in contrast to the first experiment, they did not have to make any perceptual choice. Hence, this control experiment served to compare the EEG and kinematic signals between a decision-making and a non-decision-making haptic task. It therefore allowed us to individuate the components of neural activity and active sensing that can be solely attributed to decision-making behavior.

Data recording and pre-processing

Movement kinematics (x, y coordinates of finger position) and applied forces were measured at a sampling frequency of 1000 Hz. Single-trial movement velocity waveforms were computed using the derivatives of the recorded position. During performance of the task, we also recorded EEG signals at 2048 sampling frequency using a Biosemi EEG system (ActiveTwo AD-box, 64 Ag-AgCl active electrodes, 10-10 montage). EEG recordings were preprocessed using EEGLab (Delorme and Makeig, 2004) as follows. EEG signals were first down-sampled to 1000 Hz to match movement kinematics and dynamics. Then, they were bandpass filtered to 1–50 Hz using a Hamming windowed FIR filter. To isolate the purely neural component of the EEG data, we used the following procedure: we first reduced the dimensionality of the EEG data by reconstituting the data using only the top 32 principal components derived from Principal Component Analysis (PCA). Thereafter, an Independent Component Analysis (ICA) decomposition of the data was performed using the Infomax algorithm (Bell and Sejnowski, 1995). We then used an ICA-based artifact removal algorithm called MARA (Winkler et al., 2011) to remove ICs attributed to blinks, horizontal eye movements (HEOG), muscular activity (EMG), and any loose or highly noisy electrodes. MARA assigned each IC a probability of being an artifact; we

removed components with probabilities above 0.5.

EEG2Behavior analysis

To identify correlations between the EEG recordings and the subjects' active sensory experience, we used a novel methodology, termed EEG2Beh(avior). EEG2Beh extends the previously developed framework Stim2EEG (Dmochowski et al., 2017) to make it applicable to simultaneously recorded neural activity and sensorimotor behavioral signals (see Fig. 2 for a graphical illustration of the procedure). In the following, we used finger velocity as the kinematic feature representing active sensing behavior, but we also note that using finger position yielded qualitatively very similar results.

The method is based on the temporal filtering of the velocity signals $s(t)$ and the spatial integration of EEG signals $m_i(t)$ recorded from i electrodes (Fig. 2):

$$u(t) = h(t) * s(t) , \quad v(t) = \sum_i g_i m_i(t) \qquad (1)$$

where * in the first equation denotes convolution between two signals, whereas the second equation is a weighted summation. The temporal filter $h(t)$ and spatial filter g_i are found by maximizing the correlation $\rho(u, v)$ between the filtered movement velocity $u(t)$ and the filtered EEG activity $v(t)$:

$$\rho(u, v) = \frac{\sum_t u(t) v(t)}{\sqrt{\sum_t u^2(t) v^2(t)}} \qquad (2)$$

To learn the filters that yield maximally correlated EEG and kinematic components, we performed Canonical Correlation Analysis (Hotelling, 1936; De Cheveigne et al., 2017) (CCA), which provides multiple pairs of solutions. Each pair c captures in g_{ci} a spatial filter of EEG activity and in $h_c(t)$ a temporal filter of the movement velocity. Here we chose the temporal aperture of the temporal filters to be [-1s,1s] (varying the filter aperture did not change qualitatively the results). This choice of temporal filter window allowed both positive and negative lags between the EEG and the velocity signals, which was crucial for investigating the mutual causal dependencies between the brain and the behavioral signals. In other words, by allowing the EEG signals to both precede and follow the velocity signals (within a 1s period), we could identify patterns of brain activity that both drive and are driven by the sensorimotor behavior.

To visualize the spatial distribution of neural activity associated with each filter, we computed the EEG components w using the "forward model" formalism as follows (Parra et al., 2002, 2005; Haufe et al., 2014):

$$W = R_{mm} G (G^T R_{mm} G)^{-1} \qquad (3)$$

where R_{mm} is the autocovariance matrix of the EEG data matrix $M = [m_1, m_2, \cdots, m_I$ and $G = [g_1, g_2, \cdots, g_C$ is a matrix containing the C CCA-derived spatial filters. The corresponding forward models are the columns of matrix $W = [w_1, w_2, \cdots, w_C$.

Hence this approach extracts C pairs of temporal kinematic components and spatial EEG components $(h_t, w_s)_i$ that correlate with strength ρ_i in decreasing order $\rho_1 > \rho_2 > \ldots > \rho_C$.

To determine statistical significance of the correlations at each learned component pair ($\rho_k > 0$), we randomized the phase spectrum of the EEG signals, which disrupted the temporal relationship between the EEG activity and the kinematics while preserving the autocorrelation structure of the signals (Theiler et al., 1992). We generated 1000 phase-randomized surrogates of the EEG data and computed EEG2Beh correlations with the kinematics to define the null distribution from which we estimated p-values. In contrast to a standard shuffling procedure that disrupts any coordination across EEG sensors, this phase-randomization procedure maintains the magnitude spectrum of the EEG signals, thus conserving their autocorrelation structure, which is
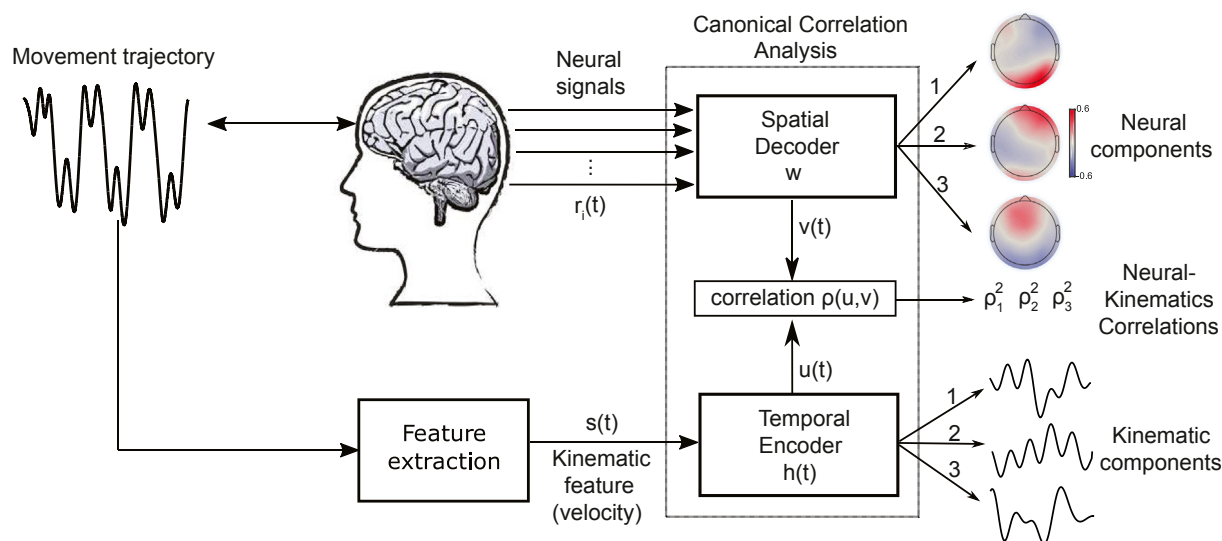
Fig. 2. Schematic view of EEG2Beh(avior) and the identified. Subjects move their fingers to actively sense a surface while their brain activity (e.g. EEG signals) $r_i(t)$ is recorded. The relevant kinematic features of the sensorimotor behavior (the movement velocity here) are extracted, resulting in a time series $s(t)$. An optimization procedure, implemented via canonical correlation analysis, then computes spatial filters w to apply to the neural signals and temporal filters $h(t)$ to apply to the velocity such that the resulting filter outputs are maximally correlated in time. The algorithm output is a set of multiple EEG-kinematic components and their coupling strengths ρ^2. Three pairs of EEG components (scalp maps of neural activity) and their matching kinematic components (temporal profiles of velocity filters) were found to show significant correlations.

a fundamental feature of the original signals when the significance of cross-correlation is assessed. Hence, using this procedure, the obtained surrogates that define the null distribution are a more plausible comparison (resulting in a stricter statistical test) than randomly shuffled surrogates.

Source localization

To identify the brain regions that generated the EEG component activations we performed a source reconstruction analysis. We used Brainstorm (Tadel et al., 2011), an open-source Matlab package for M/EEG signal processing, to translate the obtained forward models into distributions of underlying cortical activity. A standardized head model based on the average template brain of the Montreal Neurological Institute (MNI) was used as single subject MRI data were not available. To estimate the sources, we used the whitened and depth-weighted linear L2-minimum norm estimates algorithm with no noise modelling (noise covariance equal to the identity matrix) and estimated amplitude SNR of the recordings equal to 3 (default - used to compute the regularization parameter). We constrained the orientation of the source model by modelling at each grid point only one dipole that is oriented normally to the cortical surface.

Hierarchical drift diffusion modelling of performance data with EEG2Beh regressors

We fit the subjects' performance, i.e. accuracy and response time (RT), with a hierarchical drift diffusion model (HDDM) (Wabersich and Van-dekerckhove, 2014) which assumes a stochastic accumulation of sensory evidence over time, toward one of two decision boundaries corresponding to correct and incorrect choices (Ratcliff, 2002; Ratcliff and McKoon, 2008; Ratcliff et al., 2015, 2016). The model returns estimates of internal components of processing such as the rate of evidence accumulation (drift rate), the distance between decision boundaries controlling the amount of evidence required for a decision (decision boundary), a possible bias towards one of the two choices (starting point) and the duration of non-decision processes (non-decision time), which include stimulus encoding and response production. As per common practice, we assumed that stimulus differences affected the drift rate (Ratcliff and

Frank, 2012).

In short, the model iteratively adjusts the above parameters to maximize the summed log likelihood of the predicted mean response time (RT) and accuracy. The DDM parameters were estimated in a hierarchical Bayesian framework, in which prior distributions of the model parameters were updated on the basis of the likelihood of the data given the model, to yield posterior distributions (Kruschke, 2010b; Wiecki et al., 2013; Wabersich and Vandekerckhove, 2014). The use of Bayesian analysis, and specifically the hierarchical drift diffusion model has several benefits relative to traditional DDM analysis. First, posterior distributions directly convey the uncertainty associated with parameter estimates (Gelman, 2003; Kruschke, 2010a). Second, the Bayesian hierarchical framework has been shown to be especially effective when the number of observations is low (Ratcliff and Childers, 2015). Third and more importantly, this framework supports the use of other variables as regressors of the model parameters to assess relations of the model parameters with other physiological or behavioral data (Cavanagh et al., 2011, 2014; Frank et al., 2015; Nunez et al., 2015, 2017; Turner et al., 2015; Pedersen et al., 2016). This property of the HDDM allowed us to establish the link between the results of the brain-behavior coupling analysis and the decision parameters of the model.

To implement the hierarchical DDM, we used the JAGS Wiener module (Wabersich and Vandekerckhove, 2014) in JAGS (Plummer, 2003), via the Matjags interface in Matlab to estimate posterior distributions. For each trial, the likelihood of accuracy and RT was assessed by providing the Wiener first-passage time (WFPT) distribution with the four model parameters (boundary separation, starting point, non-decision time, and drift rate). Parameters were drawn from uniformly distributed priors and were estimated with non-informative mean and standard deviation group priors. The starting point was set as the midpoint between the two decision boundaries as the experimental design induced no bias towards one of the two choices (Philiastides et al., 2011). There were 5500 samples drawn from the posterior; the first 500 were discarded (as "burn-in") and the rest were subsampled ("thinned") by a factor of 50 following the conventional approach to MCMC sampling whereby initial samples are likely to be unreliable due to the selection of a random starting point and neighboring samples are likely to be highly correlated (Wiecki et al., 2013; Wabersich and Vandekerckhove, 2014). The remaining samples constituted the probability distributions of each

estimated parameter.

As part of the model fitting within the HDDM framework, we used the single-trial EEG2Beh correlations of the identified components as regressors of the decision parameters (non-decision time, τ and drift rate, δ) as follows:

$$\tau\mu = \beta_0 \quad \beta_1 * \rho_1^2 \quad \beta_2 * \rho_2^2 \quad \beta_3 * \rho_3^2 \tag{4}$$

$$\delta\mu = \gamma_0 \quad \gamma_1 * \rho_1^2 \quad \gamma_2 * \rho_2^2 \quad \gamma_3 * \rho_3^2 \tag{5}$$

In these regressions, ρ_i^2 are the squared single-trial EEG2Beh correlations of the three components respectively. The coefficients β_i (γ_i) weight the slope of the non-decision time (drift rate) by the values of ρ_i^2 on that specific trial, with an intercept β_0 (γ_0). By using these eight regression coefficients we were able to test the influences of each of the three identified components on either of the model parameters (Cavanagh et al., 2014). Posterior probability densities of each regression coefficient were estimated using the sampling procedure described above and were graphically represented as violin plots (see Fig. 4B–C for examples). Significantly positive (negative) effects were determined when >99% of the posterior density was higher (lower) than 0.

For comparison with alternate models, we used the Deviance Information Criterion (DIC), a measure widely used for fit assessment and comparison of hierarchical models (Spiegelhalter et al., 2002). DIC selects the model that achieves the best trade-off between goodness-of-fit and model complexity. Lower DIC values favor models with the highest likelihood and least degrees of freedom.

A detailed account of the analysis pipeline implemented in this study is given graphically in the form of a flowchart in Fig. 3.

Results

Tactile discrimination performance

To generate tactile stimulation that can be actively sensed, we employed a haptic stimulator (Campion et al., 2005; Frissen et al., 2012) (Fig. 1A) and programmed it to render a virtual grating texture with different amplitudes (Fig. 1B). In particular, we split the workspace of the haptic stimulator into two regions (left - L and right - R) and asked fifteen subjects to actively explore the virtual surface and report as quickly and

as accurately as possible which of the two subspaces had higher texture amplitude. One of the two regions (termed reference) had a fixed virtual amplitude while the other subspace (termed comparison) had a varying amplitude for each trial. On each trial, subjects actively moved their finger to scan the two regions in order to compare a reference texture amplitude (which was randomly presented in one of the two regions) and a comparison texture with higher or lower amplitude (six amplitude differences: 0.5, 0.25, 0.1, 0.1, 0.25 0.5) (Fig. 1C). We found that task performance improved significantly with increasing stimulus difference, as reflected by a larger fraction of correct choices ($p < 10^{-7}$, F (2, 36) = 27.03) and faster RTs ($p < 0.05$, F (2, 36) = 4.04) (Fig. 1D,F).

Active sensing behavioral kinematics

During this active tactile decision-making task, we also recorded a) the subjects' finger position, offering a detailed account of their active sensing strategy and b) their EEG activity reflecting the neural dynamics that underlie performance of this task. First, we examined what aspects of the active sensing strategy used by the subjects were affected by task difficulty. We found that subjects switched between the two textures (in order to compare their amplitudes before reaching a decision) more times when the task was harder, but this dependence of the number of crossings on stimulus differences was not significant at the population level ($p = 0.17$, F (2,36) = 1.87, Fig. 1E). Interestingly, the time-averaged speed with which the subjects scanned the textures was independent of the stimulus difference (Fig. 1G). However, instantaneous finger velocity varied considerably within each trial suggesting that subjects modulated their tactile exploration speed in order to actively sense the two surfaces before making a choice (Fig. 1H).

EEG activity

After characterizing the subjects' active sensing behavior, we aimed to investigate the structure of their whole-brain activity during performance of this task. We thus applied Principal Component Analysis (PCA) to the EEG recordings pooled across all participants to extract the main dimensions of EEG variation and then performed source localization analysis to the first three PCs to identify the neuronal origins of these brain activations. We found that the most prominent EEG components localized to premotor, motor and supplementary motor areas (first PC,
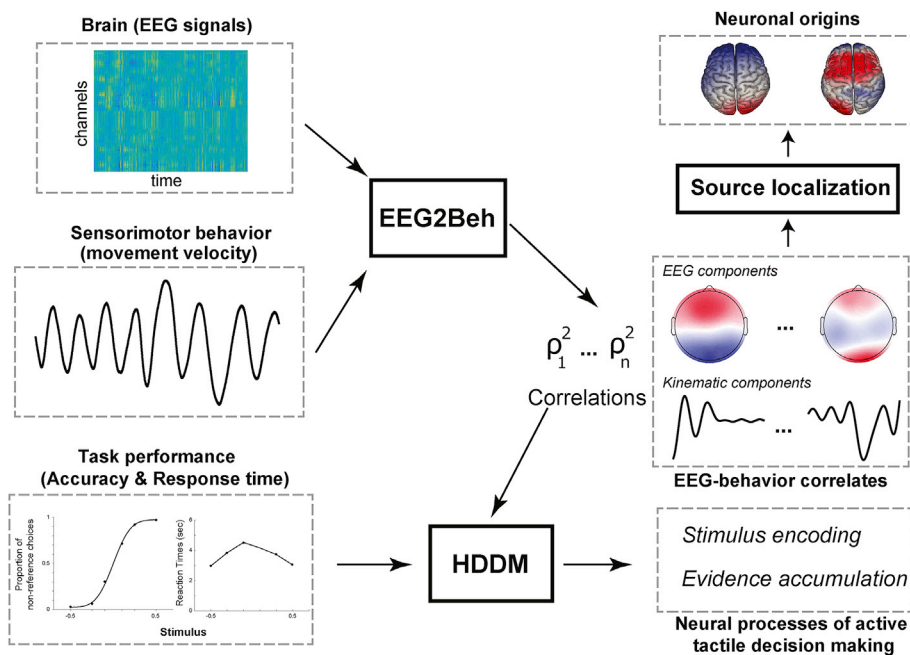

Fig. 3. Illustration of the analysis framework implemented in this study. To characterize active tactile decision-making, three types of measurements are simultaneously made: a) EEG recordings, b) sensorimotor signals (movement kinematics), and c) task performance measures (accuracy and response time - RT). EEG and kinematic signals are input to the EEG2Beh algorithm that outputs pairs of brain – behavior coupling components (scalp maps and temporal kinematic filters) and their correlation measures ρ^2. The brain (EEG) components are input to a source localization algorithm to identify their neuronal origins. The EEG2Beh coupling strengths ρ^2 inform the hierarchical drift diffusion modelling (HDDM) of the task performance data. HDDM uses the ρ^2 to translate accuracy and RT into the components of decision-making processing (such as evidence accumulation or stimulus encoding) thereby characterizing the functional role of each EEG2Beh component.

Fig. 1I), and right-lateralized somatosensory as well as other parietal areas (second and third PC, Fig. 1J-K).

Three distinct brain to active sensing couplings

Following the aforementioned general characterization of EEG activity in this task, we then probed the relationship between the subjects' brain activity and their active sensory experience. We hypothesized that the subjects' active sensing strategy is represented by their finger kinematics and in particular their movement velocity which they varied in order to actively explore the two surfaces. To relate movement velocity with the recorded EEG signals, we capitalized on a novel computational approach, termed "Stim2EEG" (Dmochowski et al., 2017), for the fusion of neuroimaging and dynamic stimulus signals. We extended the applicability of this approach to sensorimotor behavioral measurements (kinematic signals here) and termed this analytical method as "EEG2Beh(avior)". EEG2Beh aims to identify components of brain – sensorimotor behavior coupling using an optimization procedure based on Canonical Correlation Analysis (CCA) (Hotelling, 1936). Specifically, EEG2Beh selects a spatial filter w to apply to the EEG signals and a temporal filter h to apply to the kinematic feature (i.e. velocity) time series such that the resulting filter outputs are maximally correlated in time (Fig. 2). Ultimately, this approach outputs multiple spatial EEG components matched with multiple temporal kinematic components as well as the coefficient of determination (square of the correlation coefficient) of the filter outputs ρ^2, a measure of the brain-behavior coupling for each pair of components.

To identify EEG2Beh components that describe performance of this task consistently across subjects, we pooled the pre-processed EEG and velocity data across all subjects and applied them to the EEG2Beh algorithm. The algorithm extracted three pairs of distinct EEG (spatial) and kinematic (temporal) components (Fig. 2) showing significant EEG2Beh coupling ($p < 0.05$, corrected for multiple comparisons using Bonferroni correction). Source localization of the first EEG component revealed a neuronal origin in the right lateral occipital complex (LOC) (Fig. 4A). The brain source of the second EEG component was localized to the right middle frontal gyrus (MFG) (Fig. 4B), whereas the third component had its origin in the supplementary motor area (SMA) and premotor cortex (Fig. 4C). Interestingly, the first two components with the highest brain-behavior couplings did not correspond to the EEG components that accounted for the highest variance in the data (see sources of the three first PCs in Fig. 1I). This finding suggests that the components carrying most of the power in the EEG recordings did not correlate with active sensing; instead brain areas with lower activity (less than 10% of the variance of the EEG data) were more strongly coupled with the movement kinematics.

To evaluate whether the three extracted EEG2Beh components characterized the EEG-kinematics relationship for each individual subject, we filtered the single-subject EEG and velocity signals with the identified spatial and temporal filters respectively and computed the EEG2Beh correlations ρ^2 of each subject. To test for statistical significance of the single-subject correlations, we performed a permutation test using phase-randomized EEG data (see Materials and Methods for de-

tails). First, the phase-spectrum of the EEG time series of each subject was randomized and then the resulting surrogate EEG data were filtered by the spatial filters before computing the correlations with the temporally filtered velocity signals. Using this test (repeated 1000 times), we found that EEG2Beh couplings were significant ($p < 0.05$, corrected for multiple comparisons using Bonferroni correction) for all but three subjects for each component (different subjects for each component, so each subject had at least two of the three components), which suggests that the identified components were present in the majority of the subjects.

Brain-behavior correlations predict HDDM parameters

Having specified the main components of brain activity and active sensing behavior that describe this task, we then aimed to establish the missing link between this brain-behavior coupling and decision-making performance. We asked whether trial-to-trial fluctuations in the brain-behavior coupling have a direct influence on behavior and, in particular, which decision-making processes they may be implicated in. To address this question, we first quantified the brain-behavior coupling in single trials, i.e. computed single-trial ρ^2 values by filtering the single-trial EEG and kinematic data with the identified spatial and temporal filters respectively. Then, we integrated the single-trial ρ^2 values into a hierarchical drift diffusion model (HDDM) (Ratcliff and McKoon, 2008; Wiecki et al., 2013), a cognitive model of decision-making behavior that decomposes task performance, i.e. accuracy and RT, into the internal components of processing representing the rate of sensory information integration (drift rate, δ), the amount of evidence required to make a choice (decision boundary separation, α), and the duration of other processes (non-decision time, τ), i.e. stimulus encoding and response production.

As part of the fitting of the HDDM model, we estimated regression coefficients (β,) to determine the relationship between trial-to-trial variations in ρ^2 and the main decision parameters. Our hypothesis was that that the strength of the brain-behavior couplings pertains to decision formation. Hence, this approach served to assess whether any of the HDDM parameters representing distinct decision formation components showed any relation to the identified brain-behavior correlations on single trials.

Our results revealed that the task performance data were fit well by the HDDM with trial-dependent drift rate, non-decision time and decision boundary separation ($R^2 = 0.81$, see Fig. 5A for the model fits of the behavioral accuracies and RTs). This finding indicates that the HDDM model can explain behavior during such a task that, in contrast to most speeded decision-making tasks, includes active sampling and exploration of both alternatives and consequently longer response times. In particular, we found considerably longer non-decision times (1.71s 0.01s) than those typically found during rapid perceptual decisions (0.3s-0.4s), which suggests that these longer non-decision time durations likely capture the extra time needed to sense both stimuli and switch between them.

More importantly, the HDDM model with EEG2Beh regressors of the non-decision times and drift rates, provided a better trade-off between goodness-of-fit and complexity (as assessed by the Deviance Information
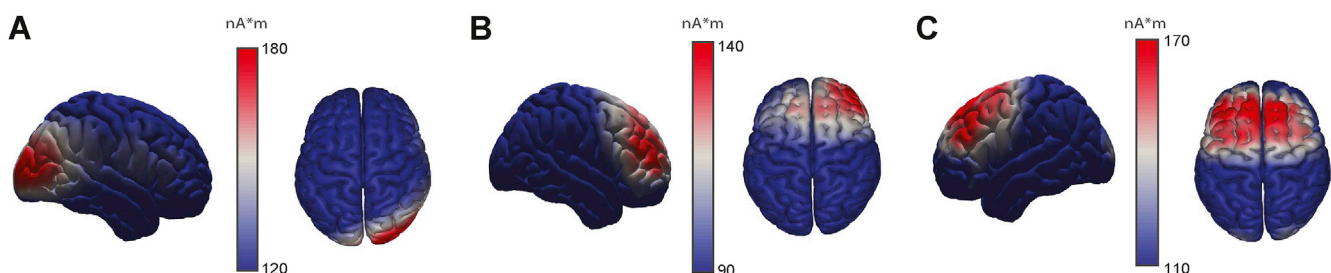

Fig. 4. Brain sources of the three EEG components showing significant brain-behavior couplings.
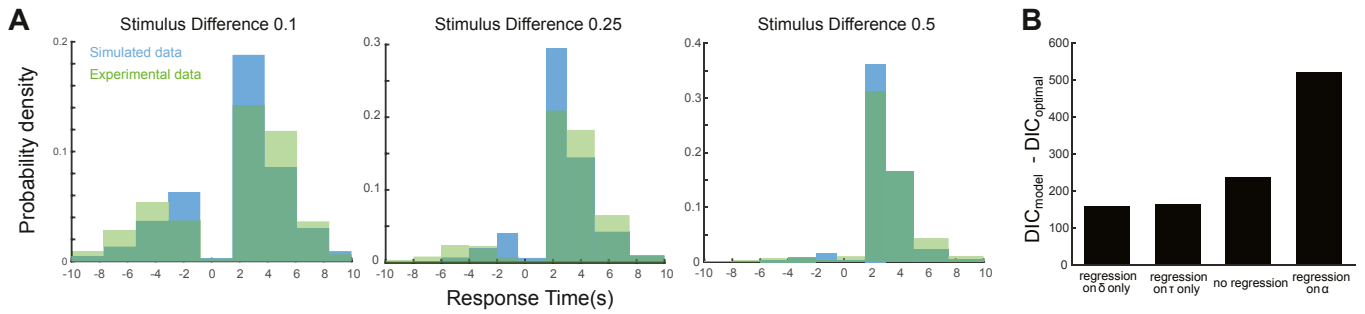
Fig. 5. HDDM fitting and model comparisons. A. Choice proportions and RT distributions are captured by EEG2Beh-informed HDDM. Behavioral RT distributions (in green) are shown for each stimulus difference together with posterior predictive simulations from the HDDM (in blue). Negative values in the time axis correspond to incorrect choices and positive values represent correct choices. Higher histogram values in the positive time axis indicate higher proportion of correct choices. Fitting accuracy is worse with lower stimulus differences. B. Comparison with alternate models. We compared the HDDM model of choice with alternative HDDM models using the Deviance Information Criterion (DIC). We tested HDDM models where either the drift rate (δ) or the non-decision time (τ) or both were not dependent on the EEG2Beh correlations and a model where the decision boundary (α) was dependent on the EEG2Beh correlations. Positive difference DIC values (DICmodel – DICoptimal) for all four models indicate that the model of choice achieved a better trade-off between goodness-of-fit and number of free parameters.

Criterion - DIC for model selection (Spiegelhalter et al., 2002)) compared to alternative HDDM models (see Fig. 5B for DIC comparisons). Specifically, the model of choice (shown in Fig. 6A) provided a better fitting of the task performance data than a) a model that did not include EEG2Beh regressors, b) models that included regressors of the non-decision times only or the drift rates only, or c) a model that included a regressor of the decision boundary separation. Thus, we deduced that using the brain-behavior couplings as predictors of single-trial non-decision times and drift rates yielded better HDDM model performance.

Central to our study, we then examined whether any of the EEG2Beh regressors were significantly predictive of the HDDM model parameters. We found that the brain-behavior correlations of the first (occipital) component were significantly negatively correlated to the non-decision times ($\beta_1 < 0$ with $p < 0.01$, i.e. the stronger the coupling the shorter the non-decision times, Fig. 6B) and the correlations of the second (prefrontal) component were predictive of the drift rate ($\gamma_2 > 0$ with $p < 0.01$, i.e. higher drift rates for stronger couplings, Fig. 6C). Interestingly, the estimated effects (γ_2) of the ρ^2 of the second component on drift rate were not significantly different for the three difficulty levels (Fig. 5C) indicating that this relationship is not modulated by the amount of sensory evidence. In contrast, the constant term (γ_0) showed a significant increase ($p < 0.001$) with the amount of sensory evidence. Taken together, these results suggest that the drift rate was proportional to the amount of sensory evidence and its trial-to-trial fluctuations were
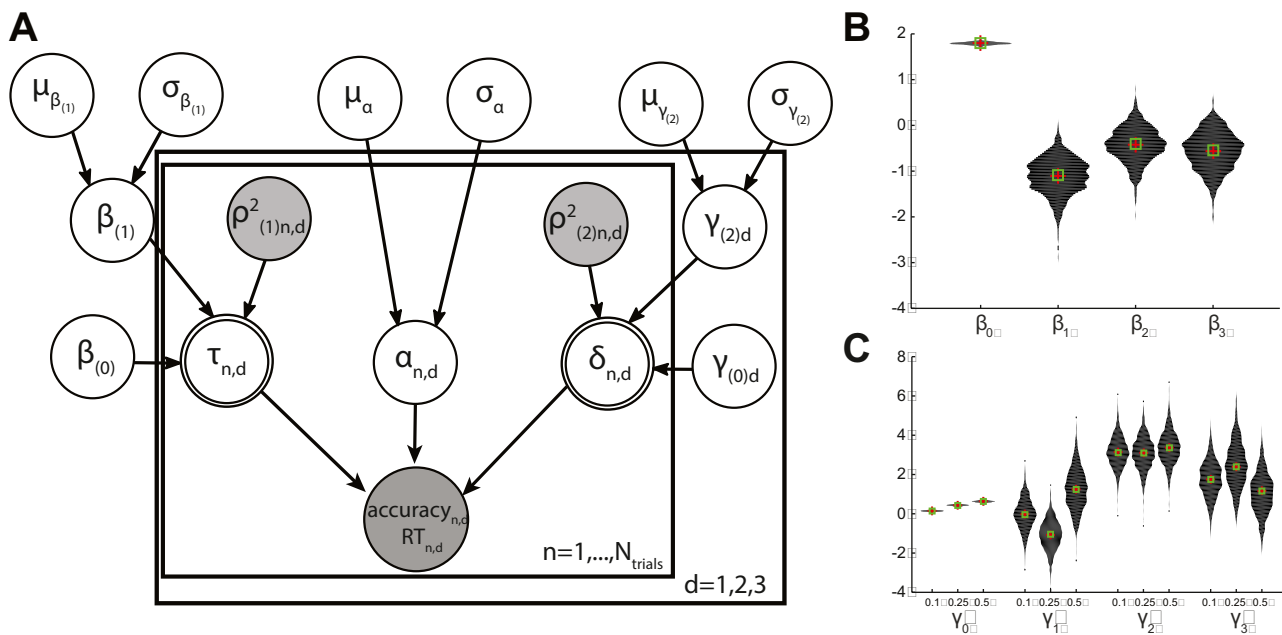

Fig. 6. Formulation of best HDDM model and regression results. A. Graphical model showing hierarchical estimation of Drift Diffusion Model parameters with EEG2Beh regressors. Round nodes represent continuous random variables and double-bordered nodes represent deterministic variables, defined in terms of other variables. Shaded nodes represent recorded or computed signals, including single-trial behavioral data (accuracy, RT) and EEG2Beh coupling measures (ρ^2). Open nodes represent unobserved latent parameters. Parameters are modelled as random variables with inferred means μ and variances σ^2. Plates denote that multiple random variables share the same parents and children. The outer plate is over difficulty levels d while the inner plate is over trials n. For example, each single-trial boundary separation $a_{n,d}$ shares the same parents $\mu_{\alpha\gamma}$ and $\sigma^2_{\alpha\gamma}$ that define the distribution across trials and difficulty levels. Single-trial variations of non-decision time $\tau\mu$ and drift rate $\delta\mu$ are determined by EEG2Beh couplings with regression coefficients β_i and γ_i. B. Violin plots showing the distribution of the regression coefficients β_i (100 samples drawn from the distribution) of the coupling strengths ρ_i^2 of the three EEG2Beh components for the prediction of single-trial non-decision times τ. C. Violin plots showing the distribution of the regression coefficients γ_i (100 samples drawn from the distribution) of the coupling strengths ρ_i^2 of the three EEG2Beh components for the prediction of single-trial drift rates δ.

modulated by the brain-behavior couplings over prefrontal areas. Finally, the third component showed similar relations to the HDDM parameters as the ones described above (negative for the non-decision times and positive for the drift rates) but none of the two were significant ($p > 0.05$).

No MFG activation when performing active sensing but not decision-making

To validate the functional roles of the identified components as revealed by the HDDM analysis, we also applied the EEG2Beh analysis to EEG and kinematic signals recorded while naïve subjects actively interrogated the same stimuli but did not have to make a perceptual choice. The obtained neural components localized to SMA (first and third component) and LOC (all three components, see Fig. 7). The presence of these activations in such a non-decision-making task corroborates their involvement in active sensing behavior. In particular, these results are consistent with the identified implication of LOC in the formation of tactile stimulus representations, i.e. a sensory/stimulus-encoding role, and a neither sensory nor decision (but likely a motor) related role for SMA. Importantly, no MFG activation was found in this control experiment which indicates that this component is present only when a perceptual choice is made and reflects a decision-related signal.

Discussion

In this study, we probed the components of brain activity and sensorimotor behavior involved in active perceptual decisions and showed that the sensorimotor strategy employed for active sensing drives the perceptual and cognitive processes leading to decision formation. In particular, the quality of tactile stimulus encoding and evidence accumulation pertains to the coupling between the kinematic patterns of the subject's motion and the neural activity that drives (and is driven by) this motion. The significance of our approach and the implications of the findings are discussed in the following.

Active sensing as a window onto the neural processes of decision-making

There has been significant progress in the study of the neural processes of perceptual decision-making (Heekeren et al., 2008; Donner et al., 2009; Rushworth et al., 2009; O'Connell et al., 2012; Wyart et al., 2012; Lou et al., 2014; Hanks and Summerfield, 2017). However, in most decision-making research, sensory information sampling, processing, and integrating takes place passively, whereas in real-world settings most perceptual decisions are made during active behaviors (e.g eye movements to gather information about a visual stimulus (Najemnik and Geisler, 2005; Kleinfeld et al., 2006; Renninger et al., 2007; Najemnik and Geisler, 2008; Navalpakkam et al., 2010; Chukoskie et al., 2013; Toscani et al., 2013) or hand/finger movements to explore a tactile surface (Lederman and Klatzky, 1986, 1987; Oddo et al., 2017; Rongala et al., 2017)). This process entails the integration of information from multiple locations in order to both select the next movement and solve the task (Hayhoe and Ballard, 2005; Rothkopf et al., 2007; Schroeder

et al., 2010; Chukoskie et al., 2013; Morillon et al., 2015; Schroeder and Ritt, 2016; Yang et al., 2016a, 2016b). Here we investigated this sensorimotor coupling in a decision making task using a novel approach which decodes a pattern of neural activity that encodes a pattern of the movement kinematics (Dmochowski et al., 2017). The development of similar approaches relating neural activity to continuous stimulus or behavioral variables has been a topic of major recent interest (Crosse et al., 2016; De Cheveigne et al., 2017; Ince et al., 2017; Oddo et al., 2017).

A distributed neural network for active perceptual decision-making

Here, we found that movement kinematics are encoded in different brain regions and the respective brain-behavior coupling was predictive of dissociable decision-making processes.

First, the coupling of right occipital cortical activity with the movement kinematics was shown to modulate the non-decision time duration of the decision formation procedure. This parameter includes the durations of a) the stimulus encoding and b) the motor response to indicate the choice made. From these two processes, the latter is not expected to vary significantly from trial to trial in this experimental paradigm and furthermore, motor actions are not localized in occipital areas. Hence, we deduce that the correlation of the first pair of EEG2Beh components is likely associated with the stimulus encoding process. We further discuss the role of visual cortex in tactile decision-making in the next section.

Second, we found that the component localizing to prefrontal cortex was predictive of the rate of evidence accumulation towards a tactile decision, which is also compatible with previous work. The prefrontal cortex has been shown to play an important role in decision-making and, in particular, it has been implicated in perceptual (but also economic) information integration (Heekeren et al., 2006; Philiastides et al., 2011; Rahnev et al., 2016; Sterzer, 2016). We should note that, in this study, the contribution of prefrontal cortex to evidence accumulation may be direct, i.e. by representing a decision variable, or indirect, i.e. by playing a role in regulating other cognitive processes such as task engagement, attention or arousal that impact on the rate at which evidence is accumulated. Also, our findings do not rule out the possibility that other brain areas – not directly related to active sensing - may contribute to regulating evidence accumulation in this task.

We also identified a third component localizing to the supplementary motor area that showed significant EEG-kinematics coupling but did not correlate with any DDM model parameter. SMA participates in producing motor behavior and has been previously demonstrated to be involved in tactile decision-making (Pleger et al., 2006) and, in particular, to correlate with perceptual sensitivity to tactile roughness (Kim et al., 2015). SMA has also been implicated in the calculation of motor plans during continuous movements (Pereira et al., 2017). We thus aim to further elucidate the role of SMA in active tactile decisions in future work involving simultaneous EEG and fMRI recordings.

Taken together, our results suggest that active perceptual decision-making is based on the interaction of different neural networks, which have complementary roles in decision formation (Philiastides et al., 2006; Philiastides and Sajda, 2007; Ploran et al., 2007; Heekeren et al.,
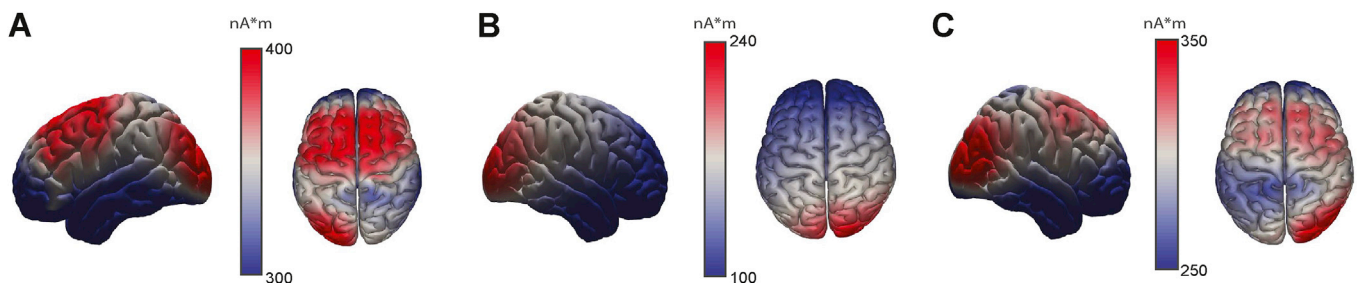

Fig. 7. Brain sources of the three significant EEG2Beh components extracted from the data of the control experiment, i.e. when subjects actively explored the tactile stimuli but did not make any perceptual choice.

2008; Mostert et al., 2015; Delis et al., 2016).

Deciphering the role of visual cortex in tactile decision-making

Our findings are consistent with prior work associating the lateral occipital cortex with tactile processing (Sathian, 2005, 2016; Zhang et al., 2005; Stilla et al., 2008; Lucan et al., 2010) and assigning a multimodal role to the visual cortex (Lacey et al., 2007; Stilla and Sathian, 2008; Lacey and Sathian, 2011, 2012, 2014, 2015; Murray, 2016; Murray et al., 2016). Importantly, Zangaladze and collaborators demonstrated the causal involvement of occipital cortex in tactile discrimination performance (Zangaladze et al., 1999). Here we investigated further its role in tactile behaviors in which decision times are under subjects' control and showed that occipital cortex contributes to the transmission of information from the sensory organs to the evidence accumulation process. In contrast to current belief that visual cortex represents the features of tactile stimuli that lead to a "tactile object" (tactile features provide explicit information about shape, orientation etc.) rather than fine grain tactile textures (as in our experiment) (Zangaladze et al., 1999), our data showed that the representation of the fine tactile textures indeed localized to visual cortex.

So why do we see visual cortex in a fine grain tactile discrimination task? We believe that the difference is due to active sensing. Previous work referenced above used very controlled, short trial-based paradigms where subjects were presented with stimuli without a need to actively sense. What is unique to our work is that the process of active sensing likely results in subjects dynamically forming a representation of the tactile surface into an object. For example, as they move their finger, exploring the fine texture enables them to integrate information so that they can represent spatial locations of the textural boundaries and the spatial extent of the textures themselves. Though subjects do not need to report those object-related properties here, having a representation of such properties enables them to potentially make more efficient decisions — e.g. using a representation of the tactile boundary to guide rapid comparisons of textural differences.

Though additional experiments are needed to investigate the interaction of the representation and the task objective (textural decision vs. object-level decision), our current work provides evidence that active sensing itself allows the brain to take simple stimuli and tasks and build more complex representations that would be of greater utility than just solving the simple task at hand.

Informed cognitive modelling to uncover latent neural processes

An important contribution of our study is the dissociation of the roles of the identified neural/kinematic patterns. This was only made possible by the joint cognitive modelling of behavioral and neural/kinematic data that linked the neural correlates of sensori-motor behavior with the cognitive processes involved in decision-making. Similar model-based cognitive neuroscience approaches have been proposed recently and have been shown to be effective in characterizing the neural underpinnings of behavioral components (Turner et al., 2015, 2017). By means of this approach, neural and other physiological measures of various cognitive processes have been identified (Ratcliff et al., 2009; Cavanagh et al., 2011, 2014; Ratcliff and Frank, 2012; Dmochowski and Norcia, 2015; Frank et al., 2015; Nunez et al., 2017). Here we asked whether the neural representations of active sensing are used to generate decision-making behavior and in particular if their trial-to-trial fluctuations affect decision-making performance. We found that the trial-to-trial variability of the brain-behavior coupling in a) occipital and b) prefrontal cortices – indexes the efficiency of a) stimulus encoding and b) integration of perceptual information respectively.

Overall, this study indicates that active sensing provides a window into understanding the patterns of brain activity and sensorimotor behavior that drive perceptual decision-making and offers the first direct evidence on the neural networks underlying active tactile decisions. In particular, we demonstrate that, during active tactile sensing, the right occipital (presumably "visual") cortex has a central role in forming tactile stimulus representations whereas the middle frontal gyrus contributes to regulating how quickly perceptual evidence accumulates towards a choice.

References

Bell, A.J., Sejnowski, T.J., 1995. An information-maximization approach to blind separation and blind deconvolution. Neural comput. 7, 1129–1159.

Campion, G., Wang, Q., Hayward, V., 2005. The Pantograph Mk-II: a haptic instrument. In: 2005 Ieee/Rsj International Conference on Intelligent Robots and Systems, vols. 1–4, pp. 723–728.

Cavanagh, J.F., Wiecki, T.V., Kochar, A., Frank, M.J., 2014. Eye tracking and pupillometry are indicators of dissociable latent decision processes. J. Exp. Psychol. General 143, 1476–1488.

Cavanagh, J.F., Wiecki, T.V., Cohen, M.X., Figueroa, C.M., Samanta, J., Sherman, S.J., Frank, M.J., 2011. Subthalamic nucleus stimulation reverses mediofrontal influence over decision threshold. Nat. Neurosci. 14, 1462–1467.

Chukoskie, L., Snider, J., Mozer, M.C., Krauzlis, R.J., Sejnowski, T.J., 2013. Learning where to look for a hidden target. Proc. Natl. Acad. Sci. U. S. A. 110 (Suppl 2), 10438–10445.

Crosse, M.J., Di Liberto, G.M., Bednar, A., Lalor, E.C., 2016. The multivariate temporal response function (mTRF) toolbox: a MATLAB toolbox for relating neural signals to continuous stimuli. Front. Hum. Neurosci. 10.

De Cheveigne, A., Wong, D., Di Liberto, G.M., Hjortkjaer, J., Slaney, M., Lalor, E.C., 2017. Decoding the Auditory Brain with Canonical Component Analysis bioRxiv 217281.

Delis, I., Onken, A., Schyns, P.G., Panzeri, S., Philiastides, M.G., 2016. Space-by-time decomposition for single-trial decoding of M/EEG activity. NeuroImage 133, 504–515.

Delorme, A., Makeig, S., 2004. EEGLAB: an open source toolbox for analysis of single-trial EEG dynamics including independent component analysis. J. Neurosci. Meth 134, 9–21.

Dmochowski, J.P., Norcia, A.M., 2015. Cortical components of reaction-time during perceptual decisions in humans. PLoS One 10 e0143339.

Dmochowski, J.P., Ki, J.J., DeGuzman, P., Sajda, P., Parra, L.C., 2017. Extracting multidimensional stimulus-response correlations using hybrid encoding-decoding of neural activity. NeuroImage.

Donner, T.H., Siegel, M., Fries, P., Engel, A.K., 2009. Buildup of choice-predictive activity in human motor cortex during perceptual decision making. Curr. Biol. 19, 1581–1585.

Frank, M.J., Gagne, C., Nyhus, E., Masters, S., Wiecki, T.V., Cavanagh, J.F., Badre, D., 2015. fMRI and EEG predictors of dynamic decision parameters during human reinforcement learning. J. Neurosci. 35, 485–494.

Frissen, I., Ziat, M., Campion, G., Hayward, V., Guastavino, C., 2012. The effects of voluntary movements on auditory-haptic and haptic-haptic temporal order judgments. Acta Psychol. (Amst) 141, 140–148.

Gelman, A., 2003. A Bayesian formulation of exploratory data analysis and goodness-of-fit testing. Int. Stat. Rev. 71, 369–382.

Hanks, T.D., Summerfield, C., 2017. Perceptual decision making in rodents, monkeys, and humans. Neuron 93, 15–31.

Haufe, S., Meinecke, F., Gorgen, K., Dahne, S., Haynes, J.D., Blankertz, B., Biessmann, F., 2014. On the interpretation of weight vectors of linear models in multivariate neuroimaging. NeuroImage 87, 96–110.

Hayhoe, M., Ballard, D., 2005. Eye movements in natural behavior. Trends Cognitive Sci. 9, 188–194.

Heekeren, H.R., Marrett, S., Ungerleider, L.G., 2008. The neural systems that mediate human perceptual decision making. Nat. Rev. Neurosci. 9, 467–479.

Heekeren, H.R., Marrett, S., Bandettini, P.A., Ungerleider, L.G., 2004. A general mechanism for perceptual decision-making in the human brain. Nature 431, 859–862.

Heekeren, H.R., Marrett, S., Ruff, D.A., Bandettini, P.A., Ungerleider, L.G., 2006. Involvement of human left dorsolateral prefrontal cortex in perceptual decision making is independent of response modality. P Natl. Acad. Sci. U. S. A. 103, 10023–10028.

Hotelling, H., 1936. Relations between two sets of variates. Biometrika 28, 321–377.

Ince, R.A., Giordano, B.L., Kayser, C., Rousselet, G.A., Gross, J., Schyns, P.G., 2017. A statistical framework for neuroimaging data analysis based on mutual information estimated via a Gaussian copula. Hum. Brain Mapp. 38, 1541–1573.

Kim, J., Chung, Y.G., Park, J.Y., Chung, S.C., Wallraven, C., Bulthoff, H.H., Kim, S.P., 2015. Decoding accuracy in supplementary motor cortex correlates with perceptual sensitivity to tactile roughness. Plos One 10.

Kleinfeld, D., Ahissar, E., Diamond, M.E., 2006. Active sensation: insights from the rodent vibrissa sensorimotor system. Curr. Opin. Neurobiol. 16, 435–444.

Kruschke, J.K., 2010a. What to believe: Bayesian methods for data analysis. Trends Cognitive Sci. 14, 293–300.

Kruschke, J.K., 2010b. Bayesian data analysis. Wires Cogn. Sci. 1, 658–676.

Lacey, S., Sathian, K., 2011. Multisensory object representation: insights from studies of vision and touch. Prog. Brain Res. 191, 165–176.

Lacey, S., Sathian, K., 2012. Representation of object form in vision and touch. In: Murray, M.M., Wallace, M.T. (Eds.), The Neural Bases of Multisensory Processes. Boca Raton (FL).

Lacey, S., Sathian, K., 2014. Visuo-haptic multisensory object recognition, categorization, and representation. Front. Psychol. 5, 730.

Lacey, S., Sathian, K., 2015. Crossmodal and multisensory interactions between vision and touch. Scholarpedia J. 10, 7957.

Lacey, S., Campbell, C., Sathian, K., 2007. Vision and touch: multiple or multisensory representations of objects? Perception 36, 1513–1521.

Lederman, S., Klatzky, R.L., 1986. Exploratory hand movements and object perception. B Psychon. Soc. 24, 322–322.

Lederman, S.J., Klatzky, R.L., 1987. Hand movements - a window into haptic object recognition. Cogn. Psychol. 19, 342–368.

Lou, B., Li, Y., Philiastides, M.G., Sajda, P., 2014. Prestimulus alpha power predicts fidelity of sensory encoding in perceptual decision making. NeuroImage 87, 242–251.

Lucan, J.N., Foxe, J.J., Gomez-Ramirez, M., Sathian, K., Molholm, S., 2010. Tactile shape discrimination recruits human lateral occipital complex during early perceptual processing. Hum. Brain Mapp. 31, 1813–1821.

Morillon, B., Hackett, T.A., Kajikawa, Y., Schroeder, C.E., 2015. Predictive motor control of sensory dynamics in auditory active sensing. Curr. Opin. Neurobiol. 31, 230–238.

Mostert, P., Kok, P., de Lange, F.P., 2015. Dissociating sensory from decision processes in human perceptual decision making. Sci. Rep. 5, 18253.

Murray, M., 2016. The multisensory function of visual cortices. Int. J. Psychophysiol. 108, 11–11.

Murray, M.M., Thelen, A., Thutd, G., Romei, V., Martuzzi, R., Matusz, P.J., 2016. The multisensory function of the human primary visual cortex. Neuropsychologia 83, 161–169.

Najemnik, J., Geisler, W.S., 2005. Optimal eye movement strategies in visual search. Nature 434, 387–391.

Najemnik, J., Geisler, W.S., 2008. Eye movement statistics in humans are consistent with an optimal search strategy. J. Vis. 8 (4), 1–14.

Navalpakkam, V., Koch, C., Rangel, A., Perona, P., 2010. Optimal reward harvesting in complex perceptual environments. Proc. Natl. Acad. Sci. U. S. A. 107, 5232–5237.

Nunez, M.D., Srinivasan, R., Vandekerckhove, J., 2015. Individual differences in attention influence perceptual decision making. Front. Psychol. 6.

Nunez, M.D., Vandekerckhove, J., Srinivasan, R., 2017. How attention influences perceptual decision making: single-trial EEG correlates of drift-diffusion model parameters. J. Math. Psychol. 76, 117–130.

O'Connell, R.G., Dockree, P.M., Kelly, S.P., 2012. A supramodal accumulation-to-bound signal that determines perceptual decisions in humans. Nat. Neurosci. 15, 1729–1735.

Oddo, C.M., Mazzoni, A., Spanne, A., Enander, J.M.D., Mogensen, H., Bengtsson, F., Camboni, D., Micera, S., Jorntell, H., 2017. Artificial spatiotemporal touch inputs reveal complementary decoding in neocortical neurons. Sci. Rep. 7.

Parra, L., Alvino, C., Tang, A., Pearlmutter, B., Yeung, N., Osman, A., Sajda, P., 2002. Linear spatial integration for single-trial detection in encephalography. Neuroimage 17, 223–230.

Parra, L.C., Spence, C.D., Gerson, A.D., Sajda, P., 2005. Recipes for the linear analysis of EEG. NeuroImage 28, 326–341.

Pedersen, M.L., Frank, M.J., Biele, G., 2016. The drift diffusion model as the choice rule in reinforcement learning. Psychonomic Bull. Rev.

Pereira, M., Sobolewski, A., Millan, J.D.R., 2017. Action monitoring cortical activity coupled to submovements. eNeuro 4.

Philiastides, M.G., Sajda, P., 2006. Temporal characterization of the neural correlates of perceptual decision making in the human brain. Cereb. Cortex 16, 509–518.

Philiastides, M.G., Sajda, P., 2007. EEG-informed fMRI reveals spatiotemporal characteristics of perceptual decision making. J. Neurosci. 27, 13082–13091.

Philiastides, M.G., Ratcliff, R., Sajda, P., 2006. Neural representation of task difficulty and decision making during perceptual categorization: a timing diagram. J. Neurosci. 26, 8965–8975.

Philiastides, M.G., Auksztulewicz, R., Heekeren, H.R., Blankenburg, F., 2011. Causal role of dorsolateral prefrontal cortex in human perceptual decision making. Curr. Biol. 21, 980–983.

Pleger, B., Ruff, C.C., Blankenburg, F., Bestmann, S., Wiech, K., Stephan, K.E., Capilla, A., Friston, K.J., Dolan, R.J., 2006. Neural coding of tactile decisions in the human prefrontal cortex. J. Neurosci. 26, 12596–12601.

Ploran, E.J., Nelson, S.M., Velanova, K., Donaldson, D.I., Petersen, S.E., Wheeler, M.E., 2007. Evidence accumulation and the moment of recognition: dissociating perceptual recognition processes using fMRI. J. Neurosci. 27, 11912–11924.

Plummer, M., 2003. JAGS: a program for analysis of Bayesian graphical models using Gibbs sampling. In: 3rd International Workshop on Distributed Statistical Computing.

Rahnev, D., Nee, D.E., Riddle, J., Larson, A.S., D'Esposito, M., 2016. Causal evidence for frontal cortex organization for perceptual decision making. Proc. Natl. Acad. Sci. U. S. A. 113, 6059–6064.

Ratcliff, R., 2002. A diffusion model account of response time and accuracy in a brightness discrimination task: fitting real data and failing to fit fake but plausible data. Psychonomic Bull. Rev. 9, 278–291.

Ratcliff, R., McKoon, G., 2008. The diffusion decision model: theory and data for two-choice decision tasks. Neural Comput. 20, 873–922.

Ratcliff, R., Frank, M.J., 2012. Reinforcement-based decision making in corticostriatal circuits: mutual constraints by neurocomputational and diffusion models. Neural comput. 24, 1186–1229.

Ratcliff, R., Childers, R., 2015. Individual Differences and Fitting Methods for the Two-choice Diffusion Model of Decision Making. Decision 2015.

Ratcliff, R., Philiastides, M.G., Sajda, P., 2009. Quality of evidence for perceptual decision making is indexed by trial-to-trial variability of the EEG. Proc. Natl. Acad. Sci. U. S. A. 106, 6539–6544.

Ratcliff, R., Smith, P.L., McKoon, G., 2015. Modeling regularities in response time and accuracy data with the diffusion model. Curr. Dir. Psychol. Sci. 24, 458–470.

Ratcliff, R., Smith, P.L., Brown, S.D., McKoon, G., 2016. Diffusion decision model: current issues anc history. Trends Cognitive Sci. 20, 260–281.

Renninger, L.W., Verghese, P., Coughlan, J., 2007. Where to look next? Eye movements reduce local uncertainty. J. Vis. 7, 6.

Rongala, U.B., Mazzoni, A., Oddo, C.M., 2017. Neuromorphic artificial touch for categorization of naturalistic textures. Ieee T Neur Net. Lear 28, 819–829.

Rothkopf, C.A., Ballard, D.H., Hayhoe, M.M., 2007. Task and context determine where you look. J. Vis. 7.

Rushworth, M.F.S., Mars, R.B., Summerfield, C., 2009. General mechanisms for making decisions? Curr. Opin. Neurobiol. 19, 75–83.

Sathian, K., 2005. Visual cortical activity during tactile perception in the sighted and the visually deprived. Dev. Psychobiol. 46, 279–286.

Sathian, K., 2016. Analysis of haptic information in the cerebral cortex. J. Neurophysiol. 116, 1795–1806.

Schroeder, C.E., Wilson, D.A., Radman, T., Scharfman, H., Lakatos, P., 2010. Dynamics of active sensing and perceptual selection. Curr. Opin. Neurobiol. 20, 172–176.

Schroeder, J.B., Ritt, J.T., 2016. Selection of head and whisker coordination strategies during goal-oriented active touch. J. Neurophysiology 115, 1797–1809.

Spiegelhalter, D.J., Best, N.G., Carlin, B.R., van der Linde, A., 2002. Bayesian measures of model complexity and fit. J. Roy. Stat. Soc. B 64, 583–616.

Sterzer, P., 2016. Moving forward in perceptual decision making. Proc. Natl. Acad. Sci. U. S. A. 113, 5771–5773.

Stilla, R., Sathian, K., 2008. Selective visuo-haptic processing of shape and texture. Hum. Brain Mapp. 29, 1123–1138.

Stilla, R., Hanna, R., Hu, X., Mariola, E., Deshpande, G., Sathian, K., 2008. Neural processing underlying tactile microspatial discrimination in the blind: a functional magnetic resonance imaging study. J. Vis. 8 (13), 11–19.

Summerfield, C., de Lange, F.P., 2014. Expectation in perceptual decision making: neural and computational mechanisms. Nat. Rev. Neurosci. 15, 745–756.

Tadel, F., Baillet, S., Mosher, J.C., Pantazis, D., Leahy, R.M., 2011. Brainstorm: a user-friendly application for MEG/EEG analysis. Comput. Intell. Neurosci. 2011, 879716.

Theiler, J., Eubank, S., Longtin, A., Galdrikian, B., Farmer, J.D., 1992. Testing for nonlinearity in time-series - the method of surrogate data. Phys. D. 58, 77–94.

Tomassini, A., D'Ausilio, A., 2017. Passive sensorimotor stimulation triggers long lasting alpha-band fluctuations in visual perception. J. Neurophysiol. jn 00496 02017.

Tomassini, A., Ambrogioni, L., Medendorp, W.P., Maris, E., 2017. Theta oscillations locked to intended actions rhythmically modulate perception. eLife 6.

Toscani, M., Valsecchi, M., Gegenfurtner, K.R., 2013. Optimal sampling of visual information for lightness judgments. Proc. Natl. Acad. Sci. U. S. A. 110, 11163–11168.

Turner, B.M., van Maanen, L., Forstmann, B.U., 2015. Informing cognitive abstractions through neuroimaging: the neural drift diffusion model. Psychol. Rev. 122, 312–336.

Turner, B.M., Forstmann, B.U., Love, B.C., Palmeri, T.J., Van Maanen, L., 2017. Approaches to analysis in model-based cognitive neuroscience. J. Math. Psychol. 76, 65–79.

Wabersich, D., Vandekerckhove, J., 2014. Extending JAGS: a tutorial on adding custom distributions to JAGS (with a diffusion model example). Behav. Res. Methods 46, 15–28.

Wiecki, T.V., Sofer, I., Frank, M.J., 2013. HDDM: hierarchical bayesian estimation of the drift-diffusion model in Python. Front. neuroinformatics 7, 14.

Winkler, I., Haufe, S., Tangermann, M., 2011. Automatic classification of artifactual ICA-components for artifact removal in EEG signals. Behavioral and brain functions : BBF 7, 30.

Wyart, V., de Gardelle, V., Scholl, J., Summerfield, C., 2012. Rhythmic fluctuations in evidence accumulation during decision making in the human brain. Neuron 76, 847–858.

Yang, S.C., Lengyel, M., Wolpert, D.M., 2016a. Active sensing in the categorization of visual patterns. eLife 5.

Yang, S.C.H., Wolpert, D.M., Lengyel, M., 2016b. Theoretical perspectives on active sensing. Curr. Opin. Behav. Sci. 11, 100–108.

Zangaladze, A., Epstein, C.M., Grafton, S.T., Sathian, K., 1999. Involvement of visual cortex in tactile discrimination of orientation. Nature 401, 587–590.

Zhang, M., Mariola, E., Stilla, R., Stoesz, M., Mao, H., Hu, X., Sathian, K., 2005. Tactile discrimination of grating orientation: fMRI activation patterns. Hum. Brain Mapp. 25, 370–377.